Quantitative assessment of population variability in hepatic drug metabolism using a perfused 3D human liver microphysiological system.

N. Tsamandouras, T. Kostrzewski, C.L. Stokes, L.G. Griffith, D.J. Hughes, M. Cirit

NT, LG, MC: Department of Biological Engineering, Massachusetts Institute of Technology, USA.

TK, DH: CN Bio Innovations, UK.

CS: Stokes Consulting, USA.

Running Title: Assessment of variability in drug metabolism with liver MPS

Corresponding Author:
Murat Cirit, PhD
Room 16-469, Building 16,
Department of Biological Engineering,
Massachusetts Institute of Technology,
77 Massachusetts Avenue,
Cambridge, Massachusetts, 02139,
USA
Email: mcirit@mit.edu
Tel: +1 617-324-7269

Number of Text Pages: 36

Number of Tables: 1

Number of Figures: 6

Number of References: 32

Number of Words in Abstract: 247

Number of Words in Introduction: 712

Number of Words in Discussion: 1478

List of nonstandard abbreviations: ACTB: actin beta, AFE: average fold error, B2M: beta-2-microglobulin, BSA: bovine serum albumin, BSEP: bile salt export pump, $CL_{int(u)}$: unbound intrinsic clearance, CYP: cytochrome P-450, CV: coefficient of variation, DMSO: dimethyl sulfoxide, ESF: empirical scaling factor, fu_{med}: fraction unbound in medium, GAPDH: glyceraldehyde-3-phosphate dehydrogenase, GST: glutathione S-transferase, HNF4α: hepatocyte nuclear factor 4 alpha, HPRT1: hypoxanthine phosphoribosyltransferase 1, IDV: inter-donor variability, IVIVE: *in vitro - in vivo* extrapolation, IWV: inter-well variability, LC-MS: liquid chromatography - mass spectometry, LDH: lactate dehydrogenase, MPS: microphysiological system, MRP2: multidrug resistance protein 2, NLME: nonlinear mixed effects, NPCs: non-parenchymal cells, NTCP: Na/Taurocholate cotransporting polypeptide, PBS: phosphate-buffered saline, PBPK: physiologically-based pharmacokinetic, PCR: polymerase chain reaction, PT: parallel-tube, QPCR: quantitative PCR, RED: rapid equilibrium dialysis, RPLP0: ribosomal protein lateral stalk subunit P0, WEM: Williams' E medium, WS: well-stirred.

Section assignment: Metabolism, Transport, and Pharmacogenomics

Abstract

In this work, we first describe the population variability in hepatic drug metabolism using cryopreserved hepatocytes from 5 different donors cultured in a perfused 3D human liver microphysiological system and then show how the resulting data can be integrated with a modeling and simulation framework to accomplish *in vitro-in vivo* translation. For each donor, metabolic depletion profiles of 6 compounds (phenacetin, diclofenac, lidocaine, ibuprofen, propranolol and prednisolone) were measured, along with metabolite formation, mRNA levels of 90 metabolism-related genes, and markers of functional viability (LDH release, albumin and urea production). Drug depletion data were analyzed with mixed effects modeling. Substantial inter-donor variability was observed with respect to gene expression levels, drug metabolism and other measured hepatocyte functions. Specifically, inter-donor variability in intrinsic metabolic clearance ranged from 24.1% for phenacetin to 66.8% for propranolol (expressed as coefficient of variation). Albumin, urea, LDH and CYP mRNA levels were identified as significant predictors of *in vitro* metabolic clearance. Predicted clearance values from the liver microphysiological system were correlated with the observed *in vivo* values. A population physiologically-based pharmacokinetic (PBPK) model was developed for lidocaine to illustrate the translation of the *in vitro* output to the observed pharmacokinetic variability *in vivo*. Stochastic simulations with this model successfully predicted the observed clinical concentration-time profiles and the associated population variability. This is the first study of population variability in drug metabolism in the context of a microphysiological system and has important implications for the use of these systems during the drug development process.

Introduction

During preclinical drug development, prediction of hepatic clearance is of significant importance to set the first in human dose and guide the selection of dosage regimens that achieve drug concentrations within the therapeutic window. However, in order to efficiently design clinical studies, it is crucial to predict hepatic drug metabolism and human pharmacokinetics, not only at the level of an "average individual" but also accounting for the associated population variability (Jamei et al., 2009).

To investigate inter-individual variability *in vitro*, drug metabolism assays must be performed independently for hepatocytes obtained from different donors and with an appropriate statistical analysis of the obtained data to estimate the inter-donor variability in intrinsic clearance disentangled from measurement error/uncertainty and any other types of variability (e.g. inter-well). Additionally, the estimate of inter-individual variability in intrinsic metabolic clearance, as assessed *in vitro*, needs to be coupled with the population variability associated with other physiological processes *in vivo* (e.g. hepatic blood flow, drug binding to plasma proteins etc.). Thus, in order to perform *in vivo* predictions at the population level, a systems pharmacology approach (Trame et al., 2016) is desirable where the *in vitro* results are integrated into population physiologically-based pharmacokinetic (PBPK) models (Rostami-Hodjegan, 2012; Jones and Rowland-Yeo, 2013; Tsamandouras et al., 2015a; Tsamandouras et al., 2015b).

Several *in vitro* systems have been traditionally applied to study drug metabolism, including human liver microsomes (Obach, 1999) and cryopreserved human hepatocyte suspensions (Brown et al., 2007). Although these systems have been very valuable in

4

drug development (Di et al., 2012) and are easy to use, they lose metabolic activity over time, hence the study of low-clearance compounds is challenging (Di and Obach, 2015; Hutzler et al., 2015). In addition, overall these *in vitro* systems tend to under-predict *in vivo* clearance (Hallifax et al., 2010). Finally, drug metabolism studies are often performed in human liver microsomes or hepatocytes, pooled from several donors. Thus, the predicted intrinsic clearance refers to an "average individual" and the associated inter-individual variability is not obtained.

Recently, new hepatic *in vitro* culture models have emerged to improve physiological responses and mitigate the rapid loss of metabolic function typically observed in culture, thus offering opportunity to improve predictions of human drug clearance, especially for low-clearance compounds. While static 2D (two-dimensional) co-cultures of hepatocytes with other cell types show some stabilization of function, a variety of 3D (three-dimensional) culture models incorporating perfusion flow exhibit prolonged viability and function under serum-free conditions (Ebrahimkhani et al., 2014). Such 3D perfused models of liver and other tissues, where microfluidic or microscale reactors are employed to control the flow of culture medium, are often termed "Microphysiological Systems (MPS)" or "Organs on Chips (OOCs). In this work, we use a particular well-developed, commercially-available microreactor system for 3D perfused liver culture, the Liverchip^{TM} (Dash et al., 2009; Domansky et al., 2010; Sarkar et al., 2015; Vivares et al., 2015). The Liverchip^{TM} comprises a scaffold that fosters formation of an array of ~0.2 mm 3D tissue structures from primary human liver cells, and an on-board microfluidic pumping system, driven by pneumatics, that precisely perfuses the scaffold with culture medium to control oxygenation and shear stress on the tissue, enabling long-term culture

with retention of physiological responses (Dash et al., 2009; Domansky et al., 2010; Vivares et al., 2015). The Liverchip^{TM} platform, seeded with hepatocytes or with mixtures of hepatocytes and non-parenchymal cells (NPCs), has been applied to analyze drug metabolism, inflammatory effects, drug-drug interactions and as a model of breast cancer metastasis to liver (Wheeler et al., 2014; Sarkar et al., 2015; Vivares et al., 2015; Long et al., 2016).

The current work firstly focuses on the *in vitro* assessment of population variability in drug metabolism and the relationship of that to variability in other phenotypic metrics such as production of liver-specific factors (e.g., albumin, urea) and expression of metabolism-related genes. *In vitro* experiments were performed in a liver microphysiological system, housed in the LiverChip^{TM} platform, utilizing hepatocytes from different donors. The ability of pooled hepatocytes to recapitulate the average phenotype across the different donors was also assessed. Since the purpose of investigating metabolism *in vitro* is to predict human pharmacokinetics, we follow up by integrating the generated data with a computational modeling and simulation framework to attempt *in vitro* to *in vivo* translation of population variability in drug metabolism.

Methods

3D hepatocyte tissue culture

All sources of chemicals and reagents used are reported in Supplementary Material (section 1.1). Cryopreserved human primary hepatocytes from 5 different donors were purchased from Life Technologies (UK). All donors (3 males, 2 females) were Caucasians spanning the 21-72 years age range. Cells were recovered according to the supplier's instructions. Viability was assessed using trypan blue exclusion and was >85% for all lots. Hepatocyte suspensions were seeded ($6x10^5$ cells per scaffold) into scaffolds housed in the LiverChip^{TM} in a total volume of 1.6 mL per compartment. Primary human hepatocytes from the 5 different donors were cultured, as well as a pooled hepatocyte sample, which contained equal numbers of cells from each of the five donors. In total, 21 wells were seeded for each donor and the pooled sample, from which 18 were intended for the drug metabolism study (6 compounds x 3 replicate wells) and 3 were intended to be sacrificed at day 6 for RNA analysis. After the initial attachment period, cells undergo morphogenesis to form an array of 3D micro-tissues within the channels of the scaffold over a period of 3 days. Cells were maintained in Williams' E medium (WEM) containing primary hepatocyte thawing and plating supplements (Life Technologies, UK) for the first day of culture. Maintenance supplements (Life Technologies, UK), which are serum-free, were used thereafter. All cultures were maintained in a standard humidified atmosphere at 37°C with 5% CO_2 and had a first complete medium change at 24 h then after a further 72 h.

Hepatocyte culture phenotypic characterization

Albumin and urea production as well as lactate dehydrogenase (LDH) release were measured before the drug metabolism study (4 days post-seeding). Albumin production was measured in supernatant using a human albumin enzyme-linked immunosorbent assay (Assay Pro, St. Charles, MO). Urea was quantified with a colorimetric assay kit (BioAssay Systems, Hayward, CA) and lactate dehydrogenase (LDH) secretion was measured using the CytoTox 96® non-radioactive cytotoxicity assay (Promega, UK). Albumin, urea and LDH were also measured post-dose at the end of the drug metabolism study (day 5 for wells treated with phenacetin; day 6 for wells treated with diclofenac, propranolol, lidocaine and ibuprofen; and day 7 for wells treated with prednisolone). At the end of the experiment, the scaffolds/tissues were removed and washed with phosphate buffered saline (PBS). Bright field images were taken using an inverted light microscope (Leica, UK).

RNA isolation and gene expression analysis

Total RNA was extracted from freshly thawed hepatocytes or from LiverChip scaffolds cultured for 6 days (run in parallel to the drug metabolism study without the addition of any drug), using TRIzol® Reagent (Ambion) and a chloroform phase separation. QPCR was performed using SYBR® Green PCR Master Mix and primers designed against transcripts related to hepatic genes of specific interest (Supplementary Material, Table S1). Samples were analyzed using a Quantstudio 6 real time PCR system (Applied Biosystems, UK). Ct values from samples were compared and normalized to GAPDH expression. Samples were also analyzed by RT^2 Profiler PCR Arrays (Qiagen, UK).

8

Reverse transcription was performed using RT^2 First Strand Kit and cDNA was analyzed by Human Drug Metabolism (PAHS-002ZC-12) RT² Profiler™ PCR Arrays. Ct values from samples were compared and normalized to the average expression across five different housekeeping genes (ACTB, B2M, GAPDH, HPRT1 and RPLP0). The QPCR and super-array data (referring to 6 and 84 genes respectively) were merged to generate a dataset of 90 genes the expression of which was investigated. The complete methods regarding RNA isolation and the gene expression analysis are provided in Supplementary Material (section 1.2).

Drug metabolism study

At day 4, six different compounds (phenacetin, diclofenac, lidocaine, ibuprofen, propranolol and prednisolone) were added as a bolus dose to the micro-tissues at a initial concentration of 1 μM during a full medium change (final volume per well was 1.8mL) and the final solvent (DMSO) concentration never exceeded 0.1% (v/v). 60 μL supernatant samples (i.e. corresponding to the extracellular compartment) were taken at pre-determined post-dose sampling times (0, 1, 4, 6 and 24 h for phenacetin; 0, 1, 4, 24 and 48 h for diclofenac, propranolol, lidocaine and ibuprofen; and 0, 4, 24, 48, 72 h for prednisolone). For the time 0 measurements, a sample was taken out from each culture well immediately (instantaneously) after the addition of the drug-containing medium to accurately evaluate the initial drug concentration in each well. All samples were analyzed for the presence of the dosed compound. Additionally, metabolite formation was measured for phenacetin (acetaminophen), diclofenac (4-OH-diclofenac), ibuprofen (2-OH-ibuprofen) and prednisolone (6β-OH-prednisolone). Extensive details regarding

sample preparation and the LC-MS/MS analysis are provided in Supplementary Material (section 1.3).

Investigation of drug binding to the platform and tissue culture medium

The compounds were also added to LiverChip wells containing no hepatocytes to analyze non-specific binding to plate components. Each well was treated in the same way as the wells containing micro-tissues. 60 μL samples were taken from these plates at 0, 1 and 48 h post-dosing and samples were treated and analyzed for the presence of the dosed compound as described in Supplementary Material (section 1.3).

Unbound drug fraction in the bovine serum albumin (BSA) containing cell culture medium was quantified by rapid equilibrium dialysis (RED). Details are provided in Supplementary Material (section 1.4).

Pharmacokinetic analysis of the drug depletion data

The drug depletion data corresponding to individual donors were analyzed with a population pharmacokinetic modeling approach using nonlinear mixed effects (NLME) modeling software (NONMEM$^{®}$ 7.3, ICON Development Solutions, Ellicott City, Maryland, USA) and the first order conditional estimation method with interaction (FOCE-I). A one-compartment pharmacokinetic model (model of mono-exponential decay) was employed to fit the drug depletion data (Eq.1)

$$C^{ijk} = C_0^{ij} \cdot e^{-\left(\frac{fu_{med} \cdot CL_{\text{int}(u)}^{ij}}{V_{med}}\right) \cdot t_{ijk}} \qquad \textbf{(Eq.1)}$$

, where C^{ijk} is the model prediction for the kth observed concentration regarding to the ith donor and the jth well, sampled at time t_{ijk}; C_0^{ij} is the substrate concentration in the media at time 0 regarding to the ith donor and the jth well (experimentally measured by sampling each well instantaneously after the addition of the drug-containing medium); V_{med} is the volume of the medium during the substrate depletion experiment (1.8 mL); fu_{med} is the fraction of drug which is unbound in the medium and thus available for metabolism (experimentally determined with equilibrium dialysis); and $CL_{\text{int}(u)}^{ij}$ is the unbound intrinsic clearance regarding to the ith donor and the jth well. Both inter-donor variability (IDV) and inter-well variability (IWV) were taken into account during the estimation of unbound intrinsic clearance using an exponential relationship (see Eq.2), which assumes that clearance is log-normally distributed.

$$CL_{\text{int}(u)}^{ij} = CL_{\text{int}(u)} \cdot e^{\eta_i + \kappa_{ij}} \qquad \textbf{(Eq.2)}$$

, where $CL_{\text{int}(u)}$ is the typical (median) value of unbound intrinsic clearance across all donors/wells; η_i is the random effect referring to between-donor differences (thus IDV) and κ_{ij} is the random effect referring to between-well differences within a donor (thus IWV). Both η and κ are assumed to be independently normally distributed with mean 0 and variance ω^2 and π^2 respectively. A common variance was assumed for all wells using the SAME option in NONMEM. Finally, an additional level of variability was taken into account, termed as residual variability (RV), using an additive error model on the scale of the log-transformed observations/predictions (see Eq.3)

11

$$\ln\left(C_{obs}^{ijk}\right) = \ln\left(C^{ijk}\right) + \varepsilon_{ijk} \qquad \textbf{(Eq.3)}$$

, where C_{obs}^{ijk} is the kth observed concentration regarding to the ith donor and the jth well, sampled at time t_{ijk}; C^{ijk} is the respective model prediction (see Eq.1); ε_{ijk} is the random effect referring to RV and thus the differences between the observed concentrations and the model predictions due to unexplained factors (e.g., measurement/assay error, model misspecification etc.); and ε is assumed to be normally distributed with mean 0 and variance σ^2. Typical goodness of fit plots (e.g. observations versus predictions, residuals versus time/predictions) and simulation-based diagnostics (e.g., visual predictive checks) were used to detect the adequacy of the developed mixed effects models (Karlsson and Savic, 2007).

The drug depletion data corresponding to the pooled hepatocytes where subsequently analyzed in a similar framework, with the difference that in the pooled hepatocytes data, the only level of variability in $CL_{int(u)}$ is the inter-well variability (IWV).

Identification of *in vitro* clearance predictors

The normalized (see Supplementary Material, section 1.5) values of intrinsic clearance obtained across different donors/wells, were investigated in relation to the values of the respective pre-dose phenotypic metrics (albumin / urea production, LDH release) and donor-specific mRNA levels of the primary for the metabolism of each compound CYP. All the methodological details regarding this investigation are provided in Supplementary Material (section 1.5).

Prediction of *in vivo* hepatic clearance

The typical value of unbound intrinsic clearance ($CL_{\text{int}(u)}$) determined for each compound from the pharmacokinetic analysis of the individual-donor *in vitro* data was subsequently used to derive a prediction with regard to the *in vivo* hepatic clearance. These predicted hepatic clearance values were then compared to clinically observed values and the overall agreement was determined by the calculation of the average fold error (AFE) across all compounds. All the related methodological details and the complete procedure (equations) used for *in vitro – in vivo* extrapolation (IVIVE) of clearance are reported in Supplementary Material (section 1.6).

Population *in vitro – in vivo* translation with the aid of PBPK modeling

A population PBPK model for lidocaine was developed, in order to illustrate the framework under which the liver MPS data can be translated to predictions of *in vivo* concentration-time profiles at the population level. The rationale for selection of lidocaine among the other *in vitro* evaluated compounds is described in Supplementary Material (section 1.7). Each tissue/organ of the developed PBPK model was assumed to be a well-stirred compartment with perfusion-limited kinetics and the liver was considered as the only site of elimination (Supplementary Material, Figure S1). Renal clearance was assumed to be negligible as only around 8% of the drug is excreted unchanged in urine (Benet et al., 2011). An empirical scaling factor (determined across all the evaluated in this work compounds) was incorporated on the *in vitro* determined hepatic clearance of lidocaine with the aim to correct for any systematic under-prediction of *in vivo* clearance with the employed *in vitro* system (Supplementary Material, sections

1.6 and 1.10). The PBPK model was mathematically described with a system of 14 mass balance differential equations (Supplementary Material, section 1.8), which were solved in Matlab R2015b (The MathWorks, Inc., Natick, Massachusetts, USA). Model simulations for 1000 "virtual individuals" were performed taking into account population variability in both the system- and drug-related parameters of the model. All model parameters along with the exact methodology for the generation of the respective population distributions are described in Supplementary Material (sections 1.9 and 1.10 for system- and drug-related parameters respectively). This approach allowed the generation of 95% population prediction intervals associated with lidocaine concentration-time profiles in arterial plasma after a constant-rate IV infusion of lidocaine HCL, 3mg/kg, over a 3-minute period. Model predictions were then compared to clinically observed arterial concentration-time profiles (Tucker and Boas, 1971) obtained under the same dosage regimen.

Results

Variability in cell culture phenotype

Human serum albumin production, urea production and LDH release to extracellular medium in the liver MPS were quantified to assess baseline cell health and phenotypic variability among the donors and wells prior to drug exposure (pre-dose, day 4). Substantial and statistically significant differences in albumin production, urea production and LDH release were observed across hepatocyte cultures from the 5 different donors (Figure 1). These phenotypic metrics were also merged across the 5 different donors and compared with the equivalent metrics from the pooled hepatocytes. Although no difference was observed in albumin production, the pooled hepatocytes were associated with higher urea production but also higher LDH levels (Figure 1).

The same phenotypic metrics were also measured at the end of the drug metabolism study (post-dose, day 5-7). Hepatocyte cultures were clearly functional throughout the study, as demonstrated by continued albumin and urea production. More specifically, across all treatments, post-dose albumin production was significantly increased and LDH release was significantly decreased compared to the equivalent pre-dose levels (Figure 2). Urea production exhibited also an overall trend of increase at post-dose measurements for all treatments except prednisolone. Further analysis supported that the above differences are likely due to the increased period in culture rather than due to a treatment (compound) effect as the post-dose metrics were not significantly different between treatments (see Supplementary Material, section 2.1). The stratification of these post-dose phenotypic metrics not only across treatments but also across different donors (Supplementary

15

Material, Figures S2-S4), indicates continued significant inter-donor variability during the drug metabolism study. Lastly, a correlation matrix plot of all the pre- and post-dose phenotypic metrics measured across all different donors (or pool of donors) and wells illustrated that strong pairwise correlations may occur across these metrics (Supplementary Material, Figure S5).

The three-dimensional micro-tissue structures were visualized at the end of the experiment. The results show that the tissue formation was consistent/comparable across the different donors and was maintained throughout the culture period (Supplementary Material, Figure S6). All the results regarding the quantitative/statistical analysis of the phenotypic metrics are described in Supplementary Material (section 2.1).

Gene expression

A comparison of gene expression (drug-metabolism related) signature between freshly thawed hepatocytes and the liver MPS showed a statistically significant difference for only 10 out of the 90 investigated genes (4 down-regulated and 6 up-regulated in the liver MPS, see Figure 3). Thus, for the vast majority of the investigated metabolism-related genes, hepatocyte micro-tissues retain gene expression (6 days after seeding) at comparable levels to that in freshly thawed hepatocytes. The list of all genes investigated in this work, the average fold-changes in expression and the associated statistical significance are reported in Supplementary Material (Table S2). In order to visualize the changes in gene expression signature separately at the level of each donor (or pool of donors) and also identify clusters of genes that are jointly up- or down-regulated, agglomerative hierarchical clustering was perfomed (Supplementary Material, Figure

16

S7). A number of genes were consistently down- or up-regulated in the liver MPS compared to freshly thawed hepatocytes for all different donors, however there were also genes that were diversely regulated across donors (some genes (e.g. CYP3A5) were strongly up-regulated in donor Hu8181 while down-regulated in all other donors). This further highlights the presence of inter-donor variability.

Additionaly, it was observed (Supplementary Material, Figure S8) that for the vast majority of genes, the magnitude of inter-donor variability in mRNA expression levels was significantly larger in freshly thawed hepatocytes (average CV across all genes was 72%) compared to the liver MPS (average CV across all genes was 34%).

Finally, out of the 90 investigated genes, only 5 in the liver MPS and none in the freshly thawed hepatocytes were significantly differentialy expressed in the pooled hepatocyte samples compared to the average values observed across the different donors (Supplementary Material, Figure S9). Thus, overall, there was no evidence against the argument that the mRNA expression levels obtained from the pooled hepatocytes can be considered as representative of the average mRNA expression obtained across the different donors. However, for the majority of genes in the liver MPS there was a non-significant trend that the pooled hepatocytes marginally over-predict the average mRNA expression obtained across the different donors, while for the majority of genes in the freshly thawed hepatocytes the opposite non-significant trend was observed (Supplementary Material, Figure S9).

Drug binding to the hepatocyte-free LiverChip and tissue culture medium

Non-specific drug binding to the hepatocyte-free LiverChip platforms was evaluated for the drugs used in metabolism studies. The quantification of each drug showed no evidence of non-specific drug binding to LiverChip components after 48-hour exposure (Supplementary Material, Figure S10). Therefore, non-specific binding of the investigated compounds to the LiverChip materials was treated as negligible in the current work.

The rapid equilibrium dialysis analysis indicated that the extent of binding to cell culture media components (e.g. BSA) varies substantially across the investigated compounds. The unbound fraction in media (fu_{med}) for diclofenac, ibuprofen, lidocaine, prednisolone, propranolol and phenacetin was determined to be 0.13 (35% CV), 0.31 (10% CV), 0.88 (9% CV), 0.94 (4% CV), 0.98 (2% CV) and 0.98 (1% CV), respectively (CV refers to coefficient of variation across triplicate experiments).

Pharmacokinetic analysis of the drug depletion data

All the drug depletion data across different donors and wells available to the pharmacokinetic analysis are presented in Figure 4 (see also Supplementary Material, section 2.2 for a numerical summary and Figure S11 for averaged concentration-time profiles for each donor across different wells). Substantial inter-donor and inter-well variability was observed in the metabolic depletion profiles of all compounds.

The results of the mixed effects modeling of the individual-donor drug depletion data are presented in Table 1. The estimates of the typical intrinsic clearance ($CL_{int(u)}$) for the 6

18

investigated compounds ranged from 0.81 μL/min/10^6 cells for prednisolone to 17.8 μL/min/10^6 cells for diclofenac. These parameters were precisely estimated for all compounds with relatively low standard errors. The intrinsic clearance of all compounds was associated with substantial inter-donor variability and the respective coefficient of variation (CV%) ranged from 24.1% for phenacetin to 66.8% for propranolol. Inter-well variability (within donor) in intrinsic clearance was less pronounced than inter-donor variability for all compounds except phenacetin (marginally higher IWV compared to IDV). The coefficient of variation respective to the inter-well variability in intrinsic clearance ranged from 6% for diclofenac to 32.9% for propranolol. The residual (unexplained) variability of the model regarding the observed concentrations was relatively small for all compounds ranging from 8.4% CV for lidocaine to 21.6% CV for propranolol.

The developed mixed effects models adequately reflect not only the average trend in the data but also the observed variability (Figure 5). Additionally, the ability of this modeling approach to accurately describe the data not only in total but also at the level of each individual donor and well is illustrated in Supplementary Material (Figure S12) in the case of propranolol (the compound with the highest degree of inter-donor and inter-well variability). The one-compartment pharmacokinetic model that was assumed for drug depletion provided an adequate description of the data, as the majority of the compounds exhibited mono-exponential declines in their concentration-time profiles, with the exception of diclofenac for which a model of bi-exponential decline might be more appropriate (Figures 4 and 5). However, additional analysis (Supplementary Material,

section 2.3) supported that the mono-exponential decline assumption for diclofenac is not introducing any substantial bias for the purpose of this work.

The results regarding to the analysis of the pooled hepatocytes drug depletion data are also presented in Table 1 and the model adequacy to describe the observed data is illustrated in Supplementary Material (Figure S13). Estimates of the typical intrinsic clearance ($CL_{int(u)}$) for the 6 investigated compounds in pooled hepatocytes ranged from 0.91 µL/min/10^6 cells for prednisolone to 18.6 µL/min/10^6 cells for diclofenac. A comparison with the equivalent clearance estimates determined from the individual-donor data indicates only minor differences (Table 1) and supports the notion that pooled hepatocytes can provide a relatively unbiased estimate of the average clearance in the donor population. More specifically, the ratio of $CL_{int(u)}$ determined in the individual donor data to the $CL_{int(u)}$ determined in the pooled hepatocytes data ranged from 0.61 for propranolol to 1.42 for ibuprofen with an average of 0.97 across all compounds (see Table 1). In addition, the 95% confidence intervals associated with this ratio included 1 for all compounds with the sole exception of propranolol, which is consequently the only compound exhibiting marginal evidence of bias in the determination of clearance in the donor population by using pooled hepatocytes.

Metabolite formation

Metabolite concentration-time profiles were determined for prednisolone, phenacetin, ibuprofen and diclofenac (Supplementary Material, Figure S14). A strong correlation was observed between the intrinsic clearance for drug depletion in a given donor/well and the respective metabolite formation levels (Supplementary Material, Figure S15). More

specifically, the linear regression R-squared values were very high for three of these compounds (0.91, 0.82 and 0.77 for prednisolone, ibuprofen and diclofenac respectively) while the correlation was weaker fon phenacetin (R-squared=0.4). These results indicate that the clear inter-donor differences observed in drug depletion clearance are also reflected in the metabolite formation levels.

Identification of *in vitro* intrinsic clearance predictors

Pre-dose albumin and urea production levels in a given donor/well were positively correlated with the respective intrinsic clearance values that were subsequently obtained from the drug metabolism study (Supplementary Material, Figure S16). On the other hand, these intrinsic clearance values were negatively correlated with the pre-dose LDH release levels, while CYP mRNA levels had only a marginal positive correlation (Supplementary Material, Figure S16). A Lasso regression model, in which several covariates are considered simultaneously, identified all the discussed above metrics (albumin, urea, LDH and CYP mRNA levels) as significant predictors of *in vitro* intrinsic clearance (Supplementary Material, Table S3 and Figure S17). Although this model was able to account for a substantial part of the observed variability in intrinsic clearance values (R-squared=0.52), there is still unexplained variability that cannot be captured solely by these 4 predictors (Supplementary Material, Figure S18).

Prediction of *in vivo* hepatic clearance

The results regarding the agreement between the observed hepatic clearances *in vivo* and the predicted hepatic clearances from the *in vitro* data are graphically illustrated and numerically summarized in Supplementary Material (Figure S19 and Table S4

respectively). Predicted clearance values from the liver MPS study were strongly correlated with the observed *in vivo* values (linear regression R-squared values of 0.75 and 0.77, respectively, when the Parallel Tube (PT) ot the Well-Stirred (WS) liver model was used). The average fold error across all compounds (under-prediction) was 4.2-fold and 4.5-fold when the PT or the WS liver model was used, respectively. The lowest degree of under-prediction was observed for phenacetin (1.7-fold and 2.1-fold for PT and WS model respectively) and the highest for propranolol (8.2-fold and 8.5-fold for PT and WS model respectively). By calculating the deviations between observations and predictions at the level of intrinsic clearances (see Supplementary Material, section 1.6), an empirical scaling factor (ESF) of 5.4 or 8.7 was derived when the PT or the WS liver model was considered, respectively.

Population *in vitro – in vivo* translation with the aid of PBPK modeling

The success of the employed population PBPK modeling approach for *in vitro-in vivo* translation at the "population level" is illustrated in Figure 6. The model predictions were in close agreement with the clinically observed data (Tucker and Boas, 1971), capturing adequately not only the average trend in the observed clinical data but also the extent of the associated inter-individual variability. Minor disagreements between model predictions and observations are considered acceptable as the model mainly utilizes *in vitro* / *in silico* information and the observed concentration-time data have not been used to fit (estimate) any of the model parameters.

Discussion

Microphysiological systems have not been fully evaluated for quantitative pharmacology applications such as prediction of hepatic drug metabolism. The current work focuses on the *in vitro* assessment of population variability in drug metabolism using a liver MPS and the subsequent translation to variability in pharmacokinetics *in vivo* using computational modeling and simulation methodologies. The overall framework employed in this work (see schematic in visual abstract) represents our recommendation with regard to the analysis and the subsequent *in vivo* translation of *in vitro* data generated in microphysiological systems.

The generated output in such systems (e.g. drug depletion profiles) is a complex function of the characteristics of the *in vitro* system (e.g. number of cells, medium volume and composition) and intrinsic biological parameters (e.g. unbound intrinsic clearance for a given drug). Through model-based analysis of the *in vitro* output, we estimated the intrinsic biological parameter (unbound intrinsic clearance) disentangled to the greatest possible degree from the *in vitro* system characteristics and any additional processes taking place into the platform (e.g. drug binding to medium components).

To estimate population variability associated with the intrinsic biological parameter, the study was designed to capture drug depletion data across multiple donors and multiple wells for each donor. The statistical analysis of such multi-level longitudinal data is challenging and can be approached with different methods. However the most suitable and unbiased method is through non-linear mixed effects (NLME) modeling (Sheiner and Beal, 1981; Sheiner and Beal, 1983; Mould and Upton, 2013), as this simultaneously

takes into account the different sources and levels of variability. It was demonstrated here that the *in vitro*-determined metabolic drug clearance varied substantially across hepatocytes from different donors. This highlights that clearance predictions for new compounds should be evaluated carefully when hepatocytes only from a single donor are used. It was also demonstrated that inter-well variability in intrinsic clearance was generally lower than the associated inter-donor variability, providing further confidence in microphysiological systems for future investigations of population variability in drug metabolism.

The unbound intrinsic clearance along with the associated inter-donor variability obtained from the liver MPS can be scaled up and integrated with the characteristics of the *in vivo* system (hepatic blood flow, organ volumes etc.) and their respective population variability through the use of PBPK modeling and the performance of stochastic simulations (Jones and Rowland-Yeo, 2013; Tsamandouras et al., 2015b; Tsamandouras et al., 2015c). The lidocaine case-study illustrated the details of this approach and to our knowledge this work is the first to combine experimental liver MPS data with a computational systems pharmacology framework to perform *in vivo* PK predictions. The accurate prediction of the clinically observed population variability in lidocaine plasma concentration-time profiles provides further confidence on the value of this combined experimental and computational approach.

Inter-donor variability was also investigated in the liver MPS with respect to additional phenotypic levels. Specifically, secreted and released biomolecules (albumin, urea, LDH) further highlighted the donor variability in terms of culture functionality and viability. Interestingly, we observed a clear correlation between the levels of these biomolecular

markers before drug administration and the subsequently determined drug clearance in the respective donors/wells. While accurate cell number quantfication in MPS technologies is a challenge, it is essential for quantitative pharmacology studies. In the current study, visual inspection of phase-contrast images indicated that seeding across different wells was consistent and equally successful across hepatocytes from different donors. In comparison the extent of the inter-donor/well differences observed in this work in drug clearance and other biomolecular metrics (albumin, urea, LDH) is much more pronounced indicating that any differences and correlations (see above) are mainly arising through the MPS biology and are not simply a reflection of differences in attached cell numbers on the scaffolds.

The mRNA expression of metabolism-related genes exhibited substantial diversity across different donors. Interestingly, inter-donor variability in mRNA expression levels was significantly lower in liver MPS cultured hepatocytes (6 days after seeding) compared to freshly thawed hepatocytes. We hypothesize that this is due to adaptation to the much more controlled and consistent enviroment of stimuli/cues (medium composition, flow, oxygen gradient etc.) present in the liver MPS culture. Finally, although CYP mRNA levels were identified in conjuction with other phenotypic metrics (albumin, urea, LDH) to be a predictor of intrinsic metabolic clearance, it accounted for only a very small portion of the clearance variability. Thus, screening mRNA expression of metabolic enzymes across different donors should not be used as a surrogate marker for inter-donor variability in metabolic activity.

The retention of hepatocyte viability and functionality in the liver MPS for the entire period of the study (up to 7 days) was also clearly demonstrated. Specifically, at the end

of drug metabolism study, not only albumin and urea were produced in high levels and LDH secretion was low, but also these metrics were substantially improved compared to pre-dose (day 4) determinations. The decrease in LDH release after few days in culture is something routinely observed in the investigated liver MPS and it is due to the adaptation of the cells in the tissue culture microenvironment. Additionally, the retention of gene expression in the liver MPS was illustrated across an array of 90 different genes including several Phase-I (e.g. CYPs) and Phase-II (e.g. GSTs) drug metabolizing enzymes together with few important hepatic regulators (e.g. HNF4a) and transporters (e.g. MRP2, BSEP, NTCP). On top of that, additional confidence on the sustained functionality of the system stems from the time dependent accumulation of drug metabolite levels across several donors/wells, while also these levels were highly correlated to the respective intrinsic clearance for the depletion of the parent drug.

In vitro drug metabolism experiments using hepatocytes that are pooled across different donors (Shibata et al., 2002) has been a common practice to avoid bias arising from inter-donor differences. However, the validity of such a practice has not previously been evaluated in MPS technologies. For the vast majority of 90 genes studied, the mRNA expression levels obtained from the pooled hepatocytes were not significantly different from the average mRNA expression levels obtained across the different donors. More importantly, by performing drug depletion studies in the liver MPS in both pooled hepatocytes or individual-donor hepatocytes, it was found that pooled hepatocytes can provide a relatively unbiased estimate of the average metabolic clearance in the donor population. Thus utilization of pooled hepatocytes to study drug metabolism in the liver

MPS is a reliable option as long as the determination of the associated inter-individual variability is not of interest.

This study focused intensively on the investigation of inter-donor variability and thus included only a small set of compounds (n=6). For this particular set of compounds, using the state of art *in vitro – in vivo* extrapolation methodologies, we obtained a robust correlation between clinically observed and predicted clearances, however in absolute values the predicted clearances were lower than those observed *in vivo* (average fold-error was 4.2 across all evaluated compounds). This trend of under-prediction is similar to that previously observed with other traditionally employed *in vitro* systems (Hallifax et al., 2010) and its origins remain a subject of ongoing research in the drug metabolism field (Galetin, 2014; Bowman and Benet, 2016). Future studies with a wide and diverse set of compounds are needed to clearly evaluate liver MPS technologies with respect to their clearance prediction capabilities and develop robust empirical relationships that can be used to correct for any under-prediction of the *in vivo* values. Finally, further work is needed on the development of mechanistic model-based methodologies to determine *in vitro* intrinsic clearance that are particularly focused on liver MPS technologies and their features.

In contrast to the traditionally employed *in vitro* systems to study drug metabolism, liver MPS technologies can be intergrated along with MPS of other organ systems allowing the development of platforms where several organ modules are interacting (Stokes et al., 2015; Yu et al., 2015). The development of such 'physiome-on-a-chip' (or human-on-a-chip) platforms is a novel and exciting research field that holds promise for significant applications in drug development (e.g. screening compounds for efficacy / toxicity) and

personalized medicine (e.g. *in vitro* clinical trials) (Fabre et al., 2014). Since the liver MPS has a central role in these platforms, the current work provides further confidence with respect to their use in pharmacokinetic / pharmacodynamic investigations.

In summary, this is the first study that specifically focuses on the *in vitro* assessment of inter-individual variability in drug metabolism in the context of a microphysiological system. It was clearly illustrated that inter-donor differences are substantial and are manifested in multiple levels (intrinsic metabolic clearance, formation of liver-specific molecules, gene expression). Moreover, this work supports the use of modeling and simulation as an indispensable tool to analyze and translate the *in vitro* results emerging from such microphysiological systems to the *in vivo* context. Finally, the current work provides further confidence regarding the use of liver MPS technologies as an alternative for drug metabolism-related investigations.

Acknowledgements

Authorship Contributions

Participated in research design: Tsamandouras, Kostrzewski, Stokes, Hughes and Cirit.

Conducted experiments: Kostrzewski.

Performed data analysis: Tsamandouras and Kostrzewski.

Contributed to the writing of the manuscript: Tsamandouras, Kostrzewski, Stokes, Griffith, Hughes and Cirit.

References

Benet LZ, Broccatelli F and Oprea TI (2011) BDDCS applied to over 900 drugs. *AAPS J* 13:519-547.

Bowman CM and Benet LZ (2016) Hepatic clearance predictions from in vitro-in vivo extrapolation and BDDCS. *Drug Metab Disposition*, doi: 10.1124/dmd.116.071514.

Brown HS, Griffin M and Houston JB (2007) Evaluation of cryopreserved human hepatocytes as an alternative in vitro system to microsomes for the prediction of metabolic clearance. *Drug Metab Disposition* 35:293-301.

Dash A, Inman W, Hoffmaster K, Sevidal S, Kelly J, Obach RS, Griffith LG and Tannenbaum SR (2009) Liver tissue engineering in the evaluation of drug safety. *Expert Opin Drug Metab Toxicol* 5:1159-1174.

Di L, Keefer C, Scott DO, Strelevitz TJ, Chang G, Bi Y-A, Lai Y, Duckworth J, Fenner K, Troutman MD and Obach RS (2012) Mechanistic insights from comparing intrinsic clearance values between human liver microsomes and hepatocytes to guide drug design. *Eur J Med Chem* 57:441-448.

Di L and Obach RS (2015) Addressing the challenges of low clearance in drug research. *AAPS J* 17:352-357.

Domansky K, Inman W, Serdy J, Dash A, Lim MHM and Griffith LG (2010) Perfused multiwell plate for 3d liver tissue engineering. *Lab on a Chip* 10:51-58.

Ebrahimkhani MR, Neiman JAS, Raredon MSB, Hughes DJ and Griffith LG (2014) Bioreactor technologies to support liver function in vitro. *Adv Drug Del Rev* 69–70:132-157.

Fabre KM, Livingston C and Tagle DA (2014) Organs-on-chips (microphysiological systems): Tools to expedite efficacy and toxicity testing in human tissue. *Exp Biol Med* 239:1073-1077.

Galetin A (2014) Rationalizing underprediction of drug clearance from enzyme and transporter kinetic data: From in vitro tools to mechanistic modeling, in *Enzyme kinetics in drug metabolism: Fundamentals and applications* (Nagar S, Argikar AU and Tweedie JD eds) pp 255-288, Humana Press, Totowa, NJ.

Hallifax D, Foster JA and Houston JB (2010) Prediction of human metabolic clearance from in vitro systems: Retrospective analysis and prospective view. *Pharm Res* 27:2150-2161.

Hutzler JM, Ring BJ and Anderson SR (2015) Low-turnover drug molecules: A current challenge for drug metabolism scientists. *Drug Metab Disposition* 43:1917-1928.

Jamei M, Dickinson GL and Rostami-Hodjegan A (2009) A framework for assessing inter-individual variability in pharmacokinetics using virtual human populations and integrating general knowledge of physical chemistry, biology, anatomy, physiology and genetics: A tale of 'bottom-up' vs 'top-down' recognition of covariates. *Drug Metab Pharmacokinet* 24:53-75.

Jones HM and Rowland-Yeo K (2013) Basic concepts in physiologically based pharmacokinetic modeling in drug discovery and development. *CPT Pharmacometrics Syst Pharmacol* 2:e63.

Karlsson MO and Savic RM (2007) Diagnosing model diagnostics. *Clin Pharmacol Ther* 82:17-20.

Long TJ, Cosgrove PA, Dunn RT, Stolz DB, Hamadeh HK, Afshari C, McBride H and Griffith LG (2016) Modeling therapeutic antibody-small molecule drug-drug interactions using a 3d perfusable human liver co-culture platform. *Drug Metab Disposition*; Sep 12, dmd.116.071456. [Epub ahead of print].

Mould DR and Upton RN (2013) Basic concepts in population modeling, simulation, and model-based drug development—part 2: Introduction to pharmacokinetic modeling methods. *CPT Pharmacometrics Syst Pharmacol* 2:1-14.

Obach RS (1999) Prediction of human clearance of twenty-nine drugs from hepatic microsomal intrinsic clearance data: An examination of in vitro half-life approach and nonspecific binding to microsomes. *Drug Metab Disposition* 27:1350-1359.

Rostami-Hodjegan A (2012) Physiologically based pharmacokinetics joined with in vitro–in vivo extrapolation of adme: A marriage under the arch of systems pharmacology. *Clin Pharmacol Ther* 92:50-61.

Sarkar U, Rivera-Burgos D, Large EM, Hughes DJ, Ravindra KC, Dyer RL, Ebrahimkhani MR, Wishnok JS, Griffith LG and Tannenbaum SR (2015) Metabolite profiling and pharmacokinetic evaluation of hydrocortisone in a perfused three-dimensional human liver bioreactor. *Drug Metab Disposition* 43:1091-1099.

Sheiner LB and Beal SL (1981) Evaluation of methods for estimating population pharmacokinetic parameters. II. Biexponential model and experimental pharmacokinetic data. *J Pharmacokinet Biopharm* 9:635-651.

Sheiner LB and Beal SL (1983) Evaluation of methods for estimating population pharmacokinetic parameters. III. Monoexponential model: Routine clinical pharmacokinetic data. *J Pharmacokinet Biopharm* 11:303-319.

Shibata Y, Takahashi H, Chiba M and Ishii Y (2002) Prediction of hepatic clearance and availability by cryopreserved human hepatocytes: An application of serum incubation method. *Drug Metab Disposition* 30:892-896.

Stokes CL, Cirit M and Lauffenburger DA (2015) Physiome-on-a-chip: The challenge of "scaling" in design, operation, and translation of microphysiological systems. *CPT Pharmacometrics Syst Pharmacol* 4:559-562.

Trame MN, Biliouris K, Lesko LJ and Mettetal JT (2016) Systems pharmacology to predict drug safety in drug development. *Eur J Pharm Sci* 94:93-95.

Tsamandouras N, Dickinson G, Guo Y, Hall S, Rostami-Hodjegan A, Galetin A and Aarons L (2015a) Development and application of a mechanistic pharmacokinetic model for simvastatin and its active metabolite simvastatin acid using an integrated population PBPK approach. *Pharm Res* 32:1864-1883.

Tsamandouras N, Rostami-Hodjegan A and Aarons L (2015b) Combining the 'bottom up' and 'top down' approaches in pharmacokinetic modelling: Fitting PBPK models to observed clinical data. *Br J Clin Pharmacol* 79:48-55.

Tsamandouras N, Wendling T, Rostami-Hodjegan A, Galetin A and Aarons L (2015c) Incorporation of stochastic variability in mechanistic population pharmacokinetic models: Handling the physiological constraints using normal transformations. *J Pharmacokinet Pharmacodyn* 42:349-373.

Tucker GT and Boas RA (1971) Pharmacokinetic aspects of intravenous regional anesthesia. *Anesthesiology* 34:538-549.

Vivares A, Salle-Lefort S, Arabeyre-Fabre C, Ngo R, Penarier G, Bremond M, Moliner P, Gallas JF, Fabre G and Klieber S (2015) Morphological behaviour and metabolic capacity of cryopreserved human primary hepatocytes cultivated in a perfused multiwell device. *Xenobiotica* 45:29-44.

Wheeler SE, Clark AM, Taylor DP, Young CL, Pillai VC, Stolz DB, Venkataramanan R, Lauffenburger D, Griffith L and Wells A (2014) Spontaneous dormancy of metastatic breast cancer cells in an all human liver microphysiologic system. *Br J Cancer* 111:2342-2350.

Yu J, Cilfone NA, Large EM, Sarkar U, Wishnok JS, Tannenbaum SR, Hughes DJ, Lauffenburger DA, Griffith LG, Stokes CL and Cirit M (2015) Quantitative systems pharmacology approaches applied to microphysiological systems (mps): Data interpretation and multi-mps integration. *CPT Pharmacometrics Syst Pharmacol* 4:585-594.

Footnotes

Reprint requests to: Murat Cirit, Room 16-469, Building 16, Department of Biological Engineering, Massachusetts Institute of Technology, 77 Massachusetts Avenue, Cambridge, Massachusetts, 02139, U.S.A. Email: mcirit@mit.edu, Tel: +1 617-324-7269 Fax: +1 617-253-2400

NT and TK had equal contribution to this work.

Legends to Figures

Figure 1. Pre-dose (measured at day 4) albumin, urea and LDH levels stratified across different donors. "Hu1601", "Hu1604", "Hu1624", "Hu8150" and "Hu8181" are lot numbers corresponding to 5 different donors. "Pooled" refers to the pool of hepatocytes and "All donors" refer to the data from all 5 donors merged together. Red lines correspond to the mean of the data, purple boxes extend the mean by ± 1 SD (standard deviation) and the pink boxes correspond to 95% confidence intervals around the mean. LDH levels are expressed in optical density (OD) units at 490nm.

Figure 2. Comparison between the pre-dose (measured at day 4) and the post-dose (measured at day 6 for diclofenac, propranol, lidocaine and ibuprofen and day 5 and 7 for phenacetin and prednisolone respectively) albumin, urea and LDH levels stratified across different treatments. Data from both the 5 donors and the pooled hepatocytes are shown. Red lines correspond to the mean of the data, purple boxes extend the mean by ± 1 SD (standard deviation) and the pink boxes correspond to 95% confidence intervals around the mean. Thin black lines connect the pre- and post-dose levels in a given donor (or pool of donors) and well. Star markers inside each subplot indicate significant differences between pre- and post-dose levels (* $p < 0.05$, ** $p < 0.01$, *** $p < 0.001$). LDH levels are expressed in optical density (OD) units at 490nm.

Figure 3. Volcano plot that illustrates the average fold-change in gene expression between the liver MPS (day 6) and freshly thawed hepatocytes along with the associated statistical significance. The $\log_2$ of the fold-change is plotted on the x-axis, thus positive values indicate up-regulation in the liver MPS compared to the freshly thawed

hepatocytes, while negative values indicate down-regulation. Genes outside the two black vertical lines are up- or down-regulated more than 3-fold. On the y-axis the $-\log_{10}$ of p-value is plotted, thus the higher values indicate stronger statistical evidence of significant difference in gene expression between the liver MPS and freshly thawed hepatocytes. The genes for which significant differences were detected after multiple testing correction are highlighted in red color and the respective gene names are reported.

Figure 4. Drug depletion data available to the pharmacokinetic analysis. "Hu1601", "Hu1604", "Hu1624", "Hu8150" and "Hu8181" are lot numbers corresponding to 5 different donors. "Pool" refers to the pool of hepatocytes from the 5 donors. The small numbers on the right of each concentration point (taking values of 1, 2 or 3) aim to distinguish different wells across the same donor (or pool of donors).

Figure 5. Visual predictive checks of the developed mixed effect models with regard to the observed individual-donor drug depletion data. Closed gray circles represent the observed concentrations in medium; highlighted with purple are the areas between the 5th and 95th percentiles of model simulations that take into account the different levels of variability (90% prediction intervals), whereas the red solid line represents their median (median prediction); the horizontal dashed black line represents the limit of quantification.

Figure 6. Population PBPK model prediction of lidocaine arterial plasma concentrations during and after a constant rate IV infusion (lidocaine HCL, 3 mg/kg for 3 minutes). The clinically observed data represented with closed grey circles have been extracted from (Tucker and Boas, 1971) across 5 different subjects. The shaded area corresponds to the

95% population prediction intervals of the model and the red line corresponds to the median model prediction. The insert plot zooms in the first 16 minutes for the purpose of clarity.

Visual abstract. Schematic overview of the framework proposed in this work with regard to the analysis and the subsequent *in vivo* translation (at the population level) of the *in vitro* liver MPS data. See Discussion for detailed explanation. IDV refers to inter-donor variability.

Tables

Table 1: Parameter estimates from the modeling of the drug depletion data

Parameter	Propranolol	Prednisolone	Phenacetin	Lidocaine	Ibuprofen	Diclofenac
Individual-donor data						
$CL_{int(u)}$ [a]	3.88 (28.6%)	0.81 (14.7%)	8.91 (12.7%)	4.38 (12.9%)	5.02 (16.2%)	17.80 (16.8%)
IDV [b]	66.8% (40.9%)	29.3% (58.1%)	24.1% (80.4%)	28.5% (38.1%)	32.6% (44.9%)	36.2% (71.5%)
IWV [b]	32.9% (62.7%)	21.5% (70.0%)	26.1% (65.2%)	11.3% (26.5%)	30.7% (55.8%)	6.0% (120.9%)
RV [b]	21.6% (56.6%)	10.3% (25.8%)	14.2% (69.8%)	8.4% (34.0%)	9.6% (29.3%)	20.0% (26.2%)
Pooled hepatocytes data						
$CL_{int(u)}$ [a]	6.34 (5.9%)	0.91 (4.0%)	9.67 (17.4%)	4.24 (3.6%)	3.54 (33.3%)	18.60 (14.4%)
IWV [b]	9.6% (50.4%)	- [c]	30.7% (41.5%)	5.9% (43.7%)	62.5% (40.0%)	23.6% (54.4%)
RV [b]	19.7% (41.1%)	11.4% (32.0%)	9.5% (40.4%)	6.9% (14.4%)	7.5% (15.8%)	16.3% (28.6%)
Individual-donor / pooled hepatocytes						
$CL_{int(u)}$ ratio [d]	0.61 (0.27, 0.97)	0.89 (0.63, 1.16)	0.92 (0.61, 1.47)	1.03 (0.77, 1.31)	1.42 (0.75, 4.20)	0.96 (0.60, 1.48)
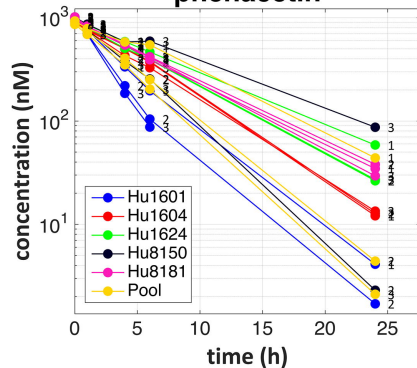
[a] The typical unbound intrinsic clearance ($CL_{int(u)}$) for each drug is reported in µL/min/10^6 cells.

[b] Inter-donor variability in unbound intrinsic clearance (IDV), inter-well variability in unbound intrinsic clearance (IWV) and the residual variability in the observed data (RV) are reported in terms of coefficient of variation (CV%), which was calculated as: $\sqrt{(e^{variance}-1)} \cdot 100$, where *variance* is the estimate of ω^2, π^2 and σ^2 for IDV, IWV and RV respectively (see Methods). Values in parentheses correspond to relative standard errors calculated as: $(standard\ error/estimate) \cdot 100$.

[c] Interwell variability could not be estimated and was fixed to 0.

[d] Ratio of $CL_{int(u)}$ determined in the individual donor data to the $CL_{int(u)}$ determined in the pooled hepatocytes data. Values in parentheses correspond to 95% confidence intervals of this ratio, calculated using the Fieller's theorem and assuming normality of the $CL_{int(u)}$ estimators. The average $CL_{int(u)}$ ratio across all compounds is 0.97.
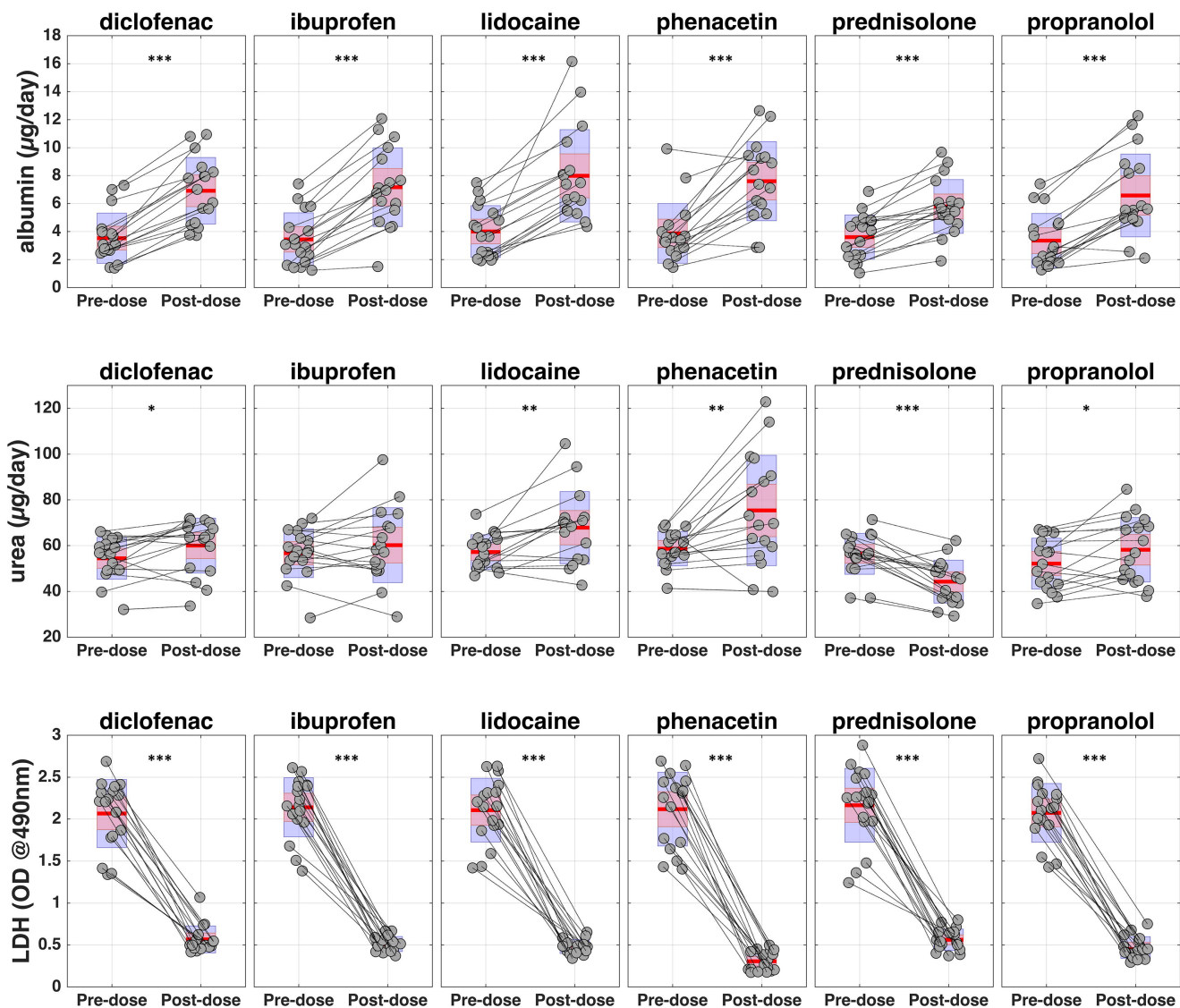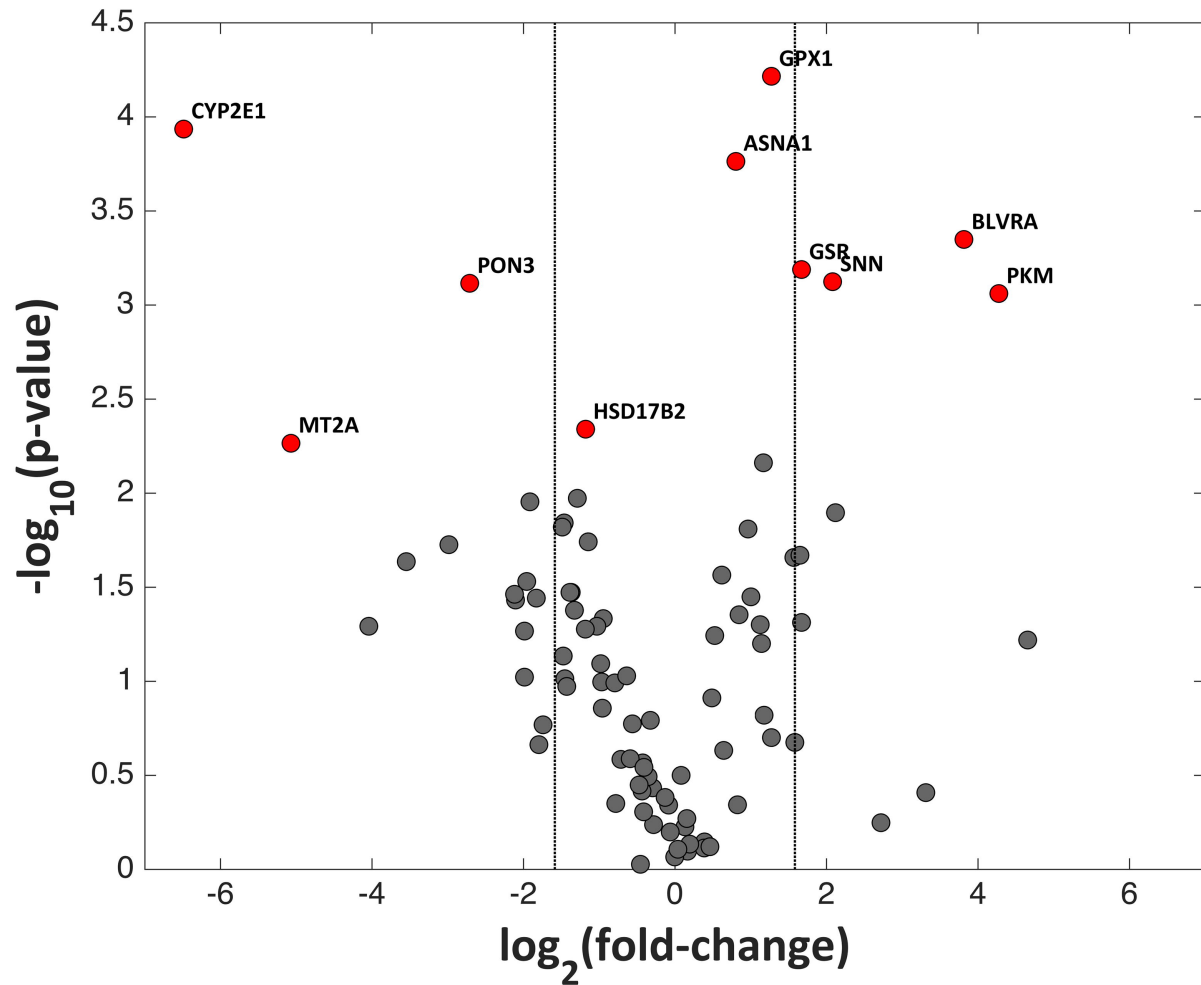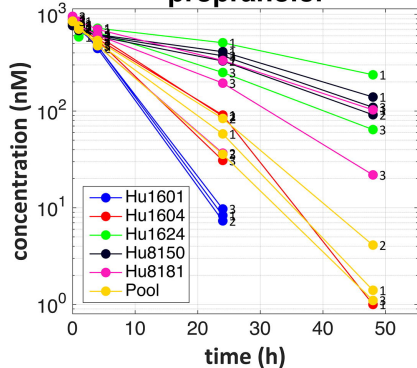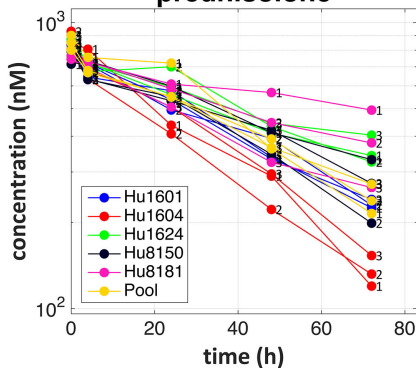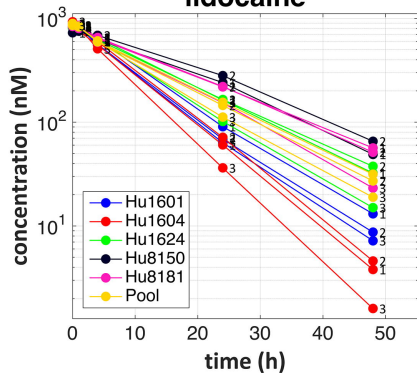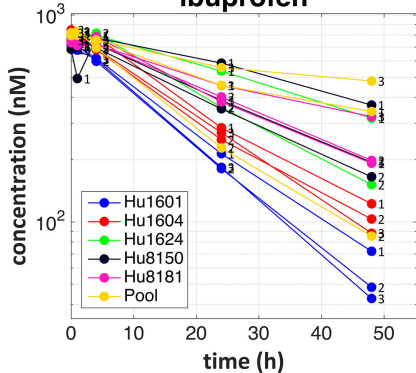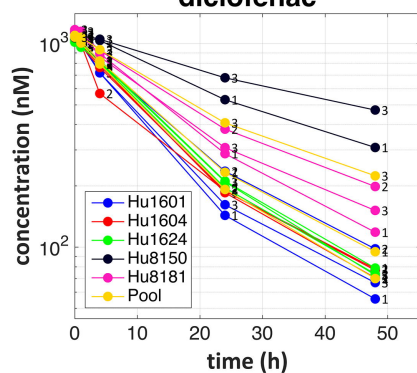
Figure 1

Pre-dose albumin production

Pre-dose urea production

Pre-dose LDH release

Figure 2

Figure 3

Figure 4

Figure 5

Figure 6